



**HAL**  
open science

# Mid infrared as a tool to study the conformational structure of starch and proteins with oil addition during gelatinization

Zeineb Nhouchi, Eliot Botosoa, Christine Chèné, Romdhane Karoui

## ► To cite this version:

Zeineb Nhouchi, Eliot Botosoa, Christine Chèné, Romdhane Karoui. Mid infrared as a tool to study the conformational structure of starch and proteins with oil addition during gelatinization. *LWT - Food Science and Technology*, 2022, 157, pp.113093. 10.1016/j.lwt.2022.113093 . hal-03653090

**HAL Id: hal-03653090**

**<https://univ-artois.hal.science/hal-03653090>**

Submitted on 22 Jul 2024

**HAL** is a multi-disciplinary open access archive for the deposit and dissemination of scientific research documents, whether they are published or not. The documents may come from teaching and research institutions in France or abroad, or from public or private research centers.

L'archive ouverte pluridisciplinaire **HAL**, est destinée au dépôt et à la diffusion de documents scientifiques de niveau recherche, publiés ou non, émanant des établissements d'enseignement et de recherche français ou étrangers, des laboratoires publics ou privés.



Distributed under a Creative Commons Attribution - NonCommercial 4.0 International License

1 **Mid infrared as a tool to study the conformational structure of starch and proteins with**  
2 **oil addition during gelatinization**

3  
4

5 **Zeineb NHOUCHI<sup>a</sup>, Eliot Patrick BOTOSOA <sup>a</sup>, Christine CHENE<sup>b</sup>, Romdhane**  
6 **KAROUI<sup>a\*</sup>**

7  
8

9 <sup>a</sup>Univ. Artois, Univ. Lille, Univ. Littoral Côte d'Opale, Univ. Picardie Jules Verne, Univ. de  
10 Liège, INRAE, Junia, UMR-T 1158, BioEcoAgro, F-62300 Lens, France

11 <sup>b</sup>ADRIANOR, F-62217, Tilloy Les Mofflaines, France

12  
13  
14  
15  
16

17 \*Correspondance author: Romdhane Karoui

18 Tel: +33 3 21 79 17 00; Fax: +33 3 21 79 17 17

19 Email: romdhane.karoui@univ-artois.fr

20

21 **Abstract**

22           The impact of varying fat and gelatinization on the starch and protein secondary  
23 structures was investigated in slurry and batter systems using mid-infrared (MIR) spectroscopy.  
24 Following the addition of both thickening agent and oil, the absorbance ratio  $R_1$ :  $1022\text{ cm}^{-1} /$   
25  $995\text{ cm}^{-1}$  ranged from 0.99 to 1.1 and from 0.85 to 0.89 for slurries and batters, respectively.  
26 The level of the  $\beta$ -turn structure decreased for both slurries (from 20.2 to 17.9 %) and batters  
27 (from 18.8 to 16.4 %) with the thickening agent addition. Similarly, oil incorporation reduced  
28 the amount of the  $\beta$ -turn structure for both slurries (from 20.2 to 9.1 %) and batters (from 18.8  
29 to 16.4 %). This result confirms the increase of the hydrophobicity of unfolded proteins, the  
30 loss of the  $\beta$ -turn structure and the increase of the  $\beta$ -sheet. The gelatinization increased the level  
31 of  $\alpha$ -helix structure and reduced the percentage of  $\beta$ -sheet structure for all slurry and batter  
32 systems in the Amide III regions.

33

34 **Keywords:** Pound cake; Starch structure; Protein secondary structure; MVAG; MIR.

35        **1. Introduction**

36        Proteins, starch, and lipids are staple macromolecules for cake batter formulation. They are  
37 responsible for the density, rheology, as well as stability of the batter (Ortiz, 2004). Jointly to  
38 starch and protein, fat components play a pivotal role in macromolecular and / or ingredients  
39 interactions influencing the baked-products quality. These interactions depend highly on the  
40 technological process, particularly mixing and baking as well as lipid structure (carbon chain  
41 length and saturation). For instance, the mixing step accelerates the formation of hydrophobic  
42 bonds of non-polar lipids with protein fractions (glutenin, gliadins, albumins), while polar lipids  
43 interact mainly with glutenin *via* hydrophilic bonds. These bonds improve the hydrogen  
44 interactions of protein fractions and provide better structural support for the gluten network  
45 (Shehzad, 2010). Furthermore, the melting of solid fat could retain air in the lipid phase of the  
46 matrix and transform the sugar-fat binary mixture into cream (Ait-Ameur, 2006). All these fat  
47 techno-functional properties depend strongly on the various crystalline forms adopted by  
48 triglycerides that define the strength of the protein-starch network (Campbell, Raikos, &  
49 Euston, 2003).

50 Campbell, Euston, and Ahmed (2016) affirmed that solid fats, such as palm oil, are known to  
51 be rich in  $\beta$  and  $\beta'$  crystalline structure, conferring dense and compact arrangement of  
52 hydrocarbon chains to the 3D protein-starch network. However, liquid oils like rapeseed oil  
53 contain mostly  $\alpha$  forms, which are known to be fragile. Moreover, oil polarity and chemical  
54 structure affect also the interfacial tension and the partitioning of the components at the  
55 interface (Devi & Khatkar, 2018). Despite all these impacts, scarce studies investigated the  
56 effect of oil types on the interactions of the ingredients during batters processing. Such  
57 information would improve baked products technologies.

58        Furthermore, the literature data showed that the simultaneous contribution of gelatinization  
59 and the interactions of the ingredients on batter structure was studied only at the macroscopic

60 scale using the micro-viscoamylograph, remaining consequently poorly understood (Hesso,  
61 Marti, et al., 2015). That is why a fine comprehension is necessary in order to perform further  
62 investigation of the involved molecular changes (Hesso, Marti et al., 2015). In this context,  
63 MIR spectroscopy is considered a powerful technique for determining protein changes during  
64 formulation, technological process, and/or storage. For instance, the technique has been  
65 successfully used for monitoring the secondary structure of proteins in: (i) milk (Ye, Zhou, Shi,  
66 Chen, & Du, 2017), (ii) egg (Duan et al., 2018), (iii) pea protein isolates (Beck, Knoerzer, &  
67 Arcot, 2017), (iv) mushroom polyphenol oxidase (Baltacıoğlu, Bayındırlı, Severcan, &  
68 Severcan, 2015) and so on. It would be interesting to investigate its potential use for monitoring  
69 proteins, lipids and starch changes during the formulation of cereal products.

70       Regarding cake batters, previous studies were focused on the study of protein secondary  
71 structure by using a simple matrix composed of gluten during mixing (Cai & Singh, 1999;  
72 Seabourn, Chung, Seib, & Mathewson, 2008) and heat treatment (Ulrichs, Drotleff, & Ternes,  
73 2015). Concerning the effect of ingredient addition on the secondary structure of baker matrix,  
74 only a few studies dealt with the impact of fiber addition (Nawrocka, Miś, & Niewiadomski,  
75 2017) and emulsifiers (Gómez, Ferrer, Añón, & Puppo, 2013) in flour system. For complex  
76 matrices, such as pound cake batter, the study of Hesso, Marti, et al. (2015) explored the effect  
77 of ingredients on the protein secondary structure by focusing mainly on the Amide I region.  
78 Thus, it would be interesting to explore other spectral regions such as the Amide III region  
79 ( $1350 - 1200 \text{ cm}^{-1}$ ), where interesting results were obtained on different proteins including  
80 lysozyme, ovalbumin, myoglobin, papain, ribonuclease A, trypsin, and so on (Cai & Singh,  
81 1999).

82 To the best of the knowledge of authors, no published work studied the simultaneous influence  
83 of the fat nature and composition on the: i) interactions between fat, starch and proteins; and ii)  
84 secondary structure of proteins before gelatinization (BG) and after gelatinization (AG).

85 Furthermore, the Amide III region was not well explored for the quantification of the secondary  
86 structure since the signal of the Amide III bands is ~5 to 10-fold weaker than that of the Amide  
87 I bands. Thus, the present work aims to investigate, for the first time, the potentiality of MIR in  
88 the 4000 – 700 cm<sup>-1</sup> region to monitor changes occurring in starch and proteins in slurry and  
89 batter systems made with different vegetable oils: palm oil (PO), rapeseed oil (RO), sunflower  
90 oil (SO) and a commercial mixture containing 60 % of sunflower oil (MO).

## 91 **2. Materials and methods**

### 92 **2.1. Materials**

93 The ingredients used for producing slurries and batters consisted of wheat flour (~15 %  
94 moisture and 13.5 % proteins contents and 25 % amylose) provided by Moulin Waast (Lille,  
95 France), PO supplied by ADM-SIO (St Laurent Blangy, France), RO, SO and MO purchased  
96 from a local supermarket (Arras, France), crystal sugar obtained from Béghin Say/Tereos (Lille,  
97 France), commercial liquid whole egg and egg yolk purchased from Fournil artesian (St Laurent  
98 Blangy, France), native starch, potassium sorbate and baking powder (Sodium Acid  
99 Pyrophosphate, baking soda and wheat starch) from Panemex S.A.S (Caden, France), salt  
100 supplied by Fournisel (St Laurent Blangy, France) and deionized water.

### 101 **2.2. Batter and slurry models preparations**

102 Model systems (S1, S2, S3, S4, B1, B2, B3, B4) were prepared (**Table 1a**) using a single-  
103 bowl mixing procedure (KitchenAid, model 5KPM5, Saint Joseph, Michigan USA), for 15 min  
104 at 400 rpm (KitchenAid Professional mixer), according to the following recipe based on the  
105 wet batter weight (wb).

106 The reference recipe is composed of wheat flour (24.5%), crystal sugar (24.5%), liquid  
107 whole egg (24.5%), fat (20.5 %), water (4%), and salt (0.4%). Since wheat was the common  
108 ingredient for all model systems and responsible for batter development, it was accurate to

109 present the composition of each model out of the weight flour basis according to their weight  
110 in the reference recipe (**Table 1b**).

111 For S4 and B4 models, the fat ingredient was replaced by an emulsion composed of 90 % of  
112 vegetable oil and a mixture of egg yolk (3 %) as an emulsifier and native starch (7 %) as a  
113 thickener. In this paper, the term “thickening agent” is used to facilitate the comprehension of  
114 the role played by egg yolk and native starch together. The use of lipid composition in models  
115 was inspired from the invention of Lecointe (2015) for replacing PO without implementing  
116 additives and providing these models with physical and rheological properties comparable to  
117 those formulated with PO.

118 All the model systems were subjected to a heat treatment using the MicroViscoAmyloGraph  
119 (MVAG) (Brabender, GmbH & Co, Duisburg, Germany) to monitor gelatinization. Thus, two  
120 model categories were respectively evaluated: slurries and batters BG and AG.

121 Regarding gelatinization, a suspension of a sample (slurry or batter) and water were accurately  
122 weighted to keep constant the moisture of the system fixed to 12 %. Suspensions were premixed  
123 and homogenized for 5 min using a pallet provided with the instrument and then transferred to  
124 the MVAG bowl. The heat treatment started from 25 to 95 °C at 7.5 °C / min, held at 95 °C for  
125 5 min, cooled from 95 to 25 °C at 7.5 °C / min, and held at 25 °C for 5 min.

### 126 **2.3.Mid infrared measurements**

127 The MIR spectra were collected at room temperature (20 °C) between 4000 and 700 cm<sup>-1</sup>  
128 at a resolution of 4 cm<sup>-1</sup> on a Fourier transform spectrometer IRTracer-100 (Shimadzu,  
129 Duisburg, Germany), which was mounted with an attenuated total reflection (ATR) accessory  
130 equipped with a grip (Pike Technologies, Inc. Madison, United States). The ATR cell was made  
131 of a horizontal ZnSe crystal which presented an incidence angle of 45 ° and a total reflection of  
132  $n = 10$ .

133 Before each measurement, the spectrum of the ZnSe crystal was recorded and used as  
134 background. H<sub>2</sub>O and CO<sub>2</sub> corrections were performed automatically by auto-adjusting the  
135 beam. Suspensions of slurry and batter models (S1, S2, S3, S4, B1, B2, B3, B4) BG and AG  
136 were placed on the crystal and pressed gently onto the crystal to assure good contact between  
137 the matrix and crystal. Between different slurry and batter samples, the crystal was carefully  
138 cleaned using ethanol and ultra-pure water. For each sample, 3 spectra were recorded within 5  
139 min of rest.

140 After spectra acquisition, the Labsolution software was deployed for arithmetic treatments.  
141 Baseline correction, normalization by the absorbance of the highest peak and deconvolution  
142 were performed before calculating area and quantifying both protein and starch structures.

#### 143 **2.4.1 Protein secondary structure determination**

144 For slurry and batter systems, the original protein spectra were used for  
145 Gaussian/Lorentzian curve-fitting. Fourier-self deconvolution and the 5-point Savitzky - Golay  
146 second-derivative function were applied according to Fevzioglu, Ozturk, Hamaker, and  
147 Campanella (2020). These treatments allowed the determination of the number of overlapped  
148 bands and their positions as well as maxima and minima of the resolved peaks, respectively on  
149 both Amide I (1600 - 1700 cm<sup>-1</sup>) and the Amide III (1200 - 1300 cm<sup>-1</sup>) regions.

150 The characteristic mean absorption frequencies of the secondary structure in proteins used in  
151 the present work are summarized in **Table 1c** according to Fevzioglu et al. (2020).

152 The secondary structure was determined from the relative area of the peaks centered at these  
153 absorption bands to Hesso, Loisel, et al. (2015). Each structure was expressed as percentages  
154 of the protein's total secondary structures in the Amide I and Amide III regions.

155 To explore deeply the evolution of secondary structure induced by ingredient interactions and  
156 gelatinization, the variation rate was calculated according to the following equation:

157 *Variation rate (%)*

$$158 = \frac{\% SS^* \text{ of any formulation} - \% SS \text{ of the formulation considered as the reference}}{\% SS \text{ of the formulation considered as the reference}}$$

159 \* *SS means secondary structures*

## 160 **2.4.2. Starch crystalline and amorphous structure determination**

161 To study the effect of the ingredient interaction and gelatinization on the starch  
162 amorphous and crystalline structures, the 800 - 1200 cm<sup>-1</sup> spectral region of raw spectra was  
163 considered, based on the study of Hesso, Marti, et al. (2015). Three absorbance ratios R<sub>1</sub> (1022  
164 cm<sup>-1</sup> / 995 cm<sup>-1</sup>), R<sub>2</sub> (1047 cm<sup>-1</sup> / 1022 cm<sup>-1</sup>) and R<sub>3</sub> (1047 cm<sup>-1</sup> / 1035 cm<sup>-1</sup>) were determined  
165 using Labsolution software provided with the ATR-FTIR spectrometer. The R<sub>1</sub> and R<sub>2</sub> ratios  
166 are known to represent the order in more crystalline regions and the state of the organization of  
167 the double helices localized inside crystallites, respectively (Flores-Morales, Jiménez-Estrada,  
168 & Mora-Escobedo, 2012), while the R<sub>3</sub> ratio is related to the modifications of crystalline  
169 structure (Copeland, Li, Niu, & Wang, 2015).

## 170 **2.4. Statistical analysis**

171 To evaluate differences (P < 0.05) between macroscopic and molecular properties of batters  
172 and slurries as a function of formulation and gelatinization, a one-way analysis of variance  
173 (ANOVA) with the least significant difference (LSD) Fisher's test was applied to the  
174 experimental data.

## 175 **3. Results and discussions**

### 176 **3.1. Impact of ingredient interactions on the starch structure during gelatinization**

177 To evaluate the effect of ingredient interactions and gelatinization on the molecular  
178 structure of amylose and amylopectin, three absorbance ratios R<sub>1</sub> (1022 cm<sup>-1</sup> / 995 cm<sup>-1</sup>), R<sub>2</sub>  
179 (1047 cm<sup>-1</sup> / 1022 cm<sup>-1</sup>) and R<sub>3</sub> (1047 cm<sup>-1</sup> / 1035 cm<sup>-1</sup>) were determined. These ratios have  
180 been defined in the literature since the R<sub>1</sub> was found to be related to the model liquid-crystalline  
181 polymeric model of the starch structure as a result of a nematic-smectic transition, while the R<sub>3</sub>

182 was found to be essentially independent to the degree of structure in the starch (Warren et al.,  
183 2016).

184 Starch crystalline and amorphous structures were found to have different trends in slurry and  
185 batter model systems. For instance, the  $R_1$  ranged between 0.99 - 1.1 and 0.85 - 0.89 for slurries  
186 and batters, respectively (**Table 2a**). Regarding the  $R_2$ , it ranged between 0.86 – 0.98 and 1.1 -  
187 1.15 for slurries and batters, respectively. A similar trend was observed for the  $R_3$ .

188 This difference could be due to a combined effect of sugar, salt, and whole egg, which  
189 determined the transition from slurry to batter. These conformational changes should be  
190 assigned to the interaction between ingredient and the availability of water. Our results were in  
191 agreement with the finding of Hesso, Marti, et al. (2015), who observed  $R_2$  and  $R_3 < 1$  for  
192 slurries while  $R_2$  and  $R_3 > 1$  for batters. A similar finding was reported by Warren et al (2013)  
193 when studying the effect of gelatinization on the  $R_1$ . The authors reported an increase of  $R_1$   
194 reflecting the transition from an ordered to a disordered state of starch structure. Additionally,  
195 they observed a greater and broader peak  $\sim 1080 \text{ cm}^{-1}$ , shifting to higher wavenumbers,  
196 associated with the crystallinity order.

197 Conjointly with gelatinization, the effect of the addition of a thickening agent (native starch  
198 + egg yolk) was assessed. The starch ratios were found to be similar in B1 (without thickening  
199 agent) model and B2 (with thickening agent) model BG and AG (**Table 2a, b**). For instance,  
200  $R_1$ ,  $R_2$  and  $R_3$  were equal to 0.94, 1 and 1.02, respectively for both B1 and B2 AG (**Table 2b**).  
201 No significant ( $P > 0.05$ ) change was observed in starch structures in slurry and batter models  
202 towards the nature of the used vegetal oil. These results could be explained by the formation of  
203 amylose-lipid complexes. Indeed, Zhou et al (2007) showed that amylose leaching increased  
204 with the addition of fatty acids. For instance, the amylose helix undergoes many conformational  
205 changes from the coil to a single, due to its interaction with fatty acids, to form the V-amylose  
206 complex. Thus, oil addition restrained the starch granule from hydration and swelling behaviors

207 during gelatinization. It could be suggested that lipids may cover the starch surface with a film,  
208 increasing hydrophobicity, the resistance to the hydrothermal treatment, and inhibiting water  
209 transfer into the granules. It is also, in agreement, with the study of Wang et al (2018) who  
210 evaluated the effect of fatty acid interactions with starch by using FTIR. No change was  
211 observed on the starch absorbance at 1022 and 1047  $\text{cm}^{-1}$ , indicating that the formation of  
212 amylopectin–fatty acid complex was too little to be detected by FTIR. Indeed, the beam  
213 penetrated the surface of the granule to a depth of 5–10 % of the granule diameter in the case  
214 of starch solution. As amylopectin is deeper due to gelatinization, spectrum intensity has been  
215 reduced, because the numerous short branches prevent or hinder the necessary helical  
216 conformation of the backbone (Guraya et al., 1997).

217 From a mechanistic side, the starch of the wheat flour used in the present study is poor in  
218 amylose. Thus, the breakage of hydrogen bonds of fatty acids in the crystalline stage and the  
219 formation of new hydrogen bonds between the carbonyl group of fatty acids and the hydroxyl  
220 group of amylose cannot be detected with FTIR. Based on this fact, it could be concluded that  
221 the thickening agent and fat would not affect the crystallinity of the batter and would not  
222 promote a fast staling.

### 223 **3.2. Impact of ingredients interactions on secondary structures of proteins in slurries** 224 **and batter before gelatinization**

225 **Figure 1a** illustrates the 1600 - 1700  $\text{cm}^{-1}$  region characteristic of the Amide I region. It  
226 showed bands located  $\sim$  1682, 1667, 1651, 1646 and 1635  $\text{cm}^{-1}$ , which have been reported in  
227 the literature when studying slurries, batters and final products such as bread and cake (Hesso,  
228 Marti, et al., 2015; Nhouchi, et al., 2018). Jointly, **Figure 1b** illustrates the 1200 - 1350  $\text{cm}^{-1}$   
229 region characteristic of the Amide III region.

230 A summary of the percentages of the different secondary structures of proteins calculated  
231 for raw ingredients (wheat flour, whole egg and yolk), as well as for slurry and batter is shown  
232 in **Table 3a**.

233 Initially, in its dry state, the wheat flour was mostly composed of the ordered secondary  
234 structure of proteins with 40.3 %, 31.6 %, 15.4 % and 12.7 % of  $\alpha$ -helix,  $\beta$ -sheet, unordered  
235 and  $\beta$ -turns, respectively. The predominance of the  $\alpha$ -helix and  $\beta$ -sheet structures in gluten  
236 could explain this trend (Bock & Damodaran, 2013). This result is quite different from the  
237 finding of Hesso, Marti, et al. (2015) who found the following order of secondary structure:  $\beta$ -  
238 sheet (59.9 %) > unordered (31.0 %) >  $\beta$ -turn (7.8 %) >  $\alpha$ -helix (1.3 %). This discrepancy could  
239 be explained by the difference in moisture and starch contents of the flours used in the recipe:  
240 15 % and 75 % of moisture and starch contents, respectively, in the present study, versus 13 %  
241 and 83 %, of moisture and starch contents, respectively in the study of Hesso et al. (2015).

242 After hydration (S1<sub>BG</sub>), the secondary structure contents of protein were modified.  
243 Indeed, in the S1 system, the  $\beta$ -sheet (51.2 %),  $\beta$ -turn (20.2 %), and unordered (18.9 %)  
244 conformations increased significantly, while the  $\alpha$ -helix conformation decreased significantly  
245 (9.6 %) in agreement with previous findings (Bock & Damodaran, 2013; Hesso, Marti, et al.,  
246 2015); the authors indicated that the competition between starch and gluten towards water  
247 generate partially hydrated gluten with a predominantly increase of  $\beta$ -sheet conformation.  
248 According to Feng et al (2018), the destruction of the  $\alpha$ -helix level might be related to the  
249 reduction of the hydrogen bond in the gluten. From a mechanistic point of view, hydration  
250 provides disulfide bonds and enhances consequently the formation of  $\beta$ -sheet.

251 To understand the effect of ingredient addition on proteins secondary structures, slurries  
252 and batters were explored in both Amide I and III regions. Surprisingly, no significant changes  
253 were observed in the Amide III region following the transition from S1<sub>BG</sub> to B1<sub>BG</sub>, where values  
254 varied for unordered (23.1 % for S1<sub>BG</sub> – 23.0 % for B1<sub>BG</sub>),  $\alpha$ -helix (8.7 % for both),  $\beta$ -sheet

255 (37.8 % for S1<sub>BG</sub> – 38.0 % for B1<sub>BG</sub>), and  $\beta$ -turn (30.4 % for S1<sub>BG</sub> – 30.0 % for B1<sub>BG</sub>) structures  
256 (**Table 3b**). This discordance between the findings in the Amide I and the Amide III regions  
257 could be explained by the difference in protein sensitivity regarding infrared radiation as  
258 showed by Bock and Damodaran (2013).

259 Moreover, the transition from S1<sub>BG</sub> to S2<sub>BG</sub> by the addition of yolk and native starch  
260 increased slightly for  $\beta$ -sheet structure from 51.2 % (S1<sub>BG</sub>) to 52.8 % (S2<sub>BG</sub>), and  $\alpha$ -helix  
261 structure from 9.6 % (S1<sub>BG</sub>) to 10.9 % (S2<sub>BG</sub>). As expected, an opposite trend was observed for  
262 the unordered and the  $\beta$ -turn structures (**Table 3a**). Similar results were found in the Amide III  
263 region, where the addition of the thickening agents allowed a classification according the  
264 following order for S1<sub>BG</sub> ( $\beta$ -sheet (37.8 %) >  $\beta$ -turn (30.4 %) > unordered (23.3%) >  $\alpha$ -helix  
265 (8.7%)) and S2<sub>BG</sub> ( $\beta$ -sheet (37.5 %) >  $\beta$ -turn (30.3 %) > unordered (23.2%) >  $\alpha$ -helix (9%))  
266 (**Table 3b**). These modifications in the secondary structure could be explained by egg and flour  
267 proteins interactions.

268 Mechanistically, the interaction between egg proteins and flour proteins could reflect also  
269 the new rearrangement of the secondary structures due to the use of yolk, where its secondary  
270 structure showed the following order:  $\beta$ -sheet (51.5 %) > unordered (19.4 %) >  $\alpha$ -helix (17.7  
271 %) >  $\beta$ -turn (11.4 %) (**Table 3a**). Luo et al. (2016) confirmed the impact of egg proteins-gluten  
272 interactions on the  $\beta$ -sheet structure. Indeed, the authors reported an increase in  $\beta$ -sheet that  
273 could be interpreted as the formation of a range of new  $\beta$ -sheet structures together with a shift  
274 to weaker hydrogen-bonded structures.

275 It should be noticed that the sugar and salt addition would not have a significant impact on the  
276 protein structures, in concordance with the findings of Secundo and Guerrieri (2005) and  
277 Widjanarko, Nugroho, and Estiasih (2011) since they might not have access to the buried parts  
278 of the molecule of gluten because of a steric hindrance.

279 The effect of oil addition BG and AG was also studied in the present study. Regardless of  
280 oil type, the unordered structure increased after the addition of fat reaching values varying  
281 between 20.2 % for S3(PO)<sub>BG</sub> and 25 % for S3(SO)<sub>BG</sub>, while  $\beta$ -turn structure decreased (9.1 %  
282 for S3(SO)<sub>BG</sub> - 19.1 % for S3(RO)<sub>BG</sub>) in comparison with the reference slurry S1<sub>BG</sub> (18.9 % and  
283 20.2 % for unordered and  $\beta$ -turn structures, respectively (**Table 3a**).

284 Regarding the  $\alpha$ -helix structure, an increase was observed after the addition of oil for S3  
285 systems except for S3(PO)<sub>BG</sub> in comparison with the reference S1<sub>BG</sub> (9.6 %). Indeed, the amount  
286 of  $\alpha$ -helix followed this order: S3(PO)<sub>BG</sub> (6.7 %) < S3(RO)<sub>BG</sub> (9.9 %) < S3(MO)<sub>BG</sub> (13.1 %) <  
287 S3(SO)<sub>BG</sub> (14.4 %). It seems that PO influenced particularly the  $\alpha$ -helix structure probably due  
288 to its richness in palmitic acid (45 %) as presented previously.

289 Concerning the  $\beta$ -sheet structure, different behaviors were observed as a function of oil type  
290 in comparison with S1<sub>BG</sub> (51.2 %). Indeed, the amount of  $\beta$ -sheet structure increased for  
291 S3(PO)<sub>BG</sub> (54.9 %) and S3(SO)<sub>BG</sub> (51.6 %), whereas it decreased for both S3(RO)<sub>BG</sub> (50.4 %)  
292 and S3(MO)<sub>BG</sub> (50.6 %) (**Table 3a**). The presence of a high level of polyunsaturated fatty acids  
293 such as linolenic acid appeared to affect significantly the variation of  $\beta$ -sheet structure content  
294 in the Amide I region when compared to S3(PO)<sub>BG</sub>. These variations were also oil botanical  
295 type-dependent in the Amide III region (**Table 3b**).

296 Regarding the Amide I region with S4 models, the addition of vegetable oil (PO, RO, SO  
297 and MO) generated different behaviors for the secondary structures (**Table 3a**). These results  
298 were in agreement with the findings of Hesso, Marti, et al. (2015) who reported an increase of  
299  $\alpha$ -helix structure from 16 % to 35 % and a decrease in  $\beta$ -sheet structure (from 49 % to 22 %)  
300 for slurry systems. An explanation could arise from the role of fat in promoting the decrease of  
301 the interactions among hydrophilic molecules and restrict the gluten–water interaction (Sivam,  
302 Sun-Waterhouse, Perera, & Waterhouse, 2013).

303 Concerning batters, to understand in-depth, the impact BG of the addition of vegetable fat  
304 in comparison with the reference formulations (B1<sub>BG</sub> or B2<sub>BG</sub>) which are considered as fat-free,  
305 it is worthy to calculate the variation rate of discrepancy between the secondary structures of  
306 B1<sub>BG</sub> or B2<sub>BG</sub> as reference and B3<sub>BG</sub> or B4<sub>BG</sub> on the basis of the secondary structure amount  
307 exhibited due to the transition of B1<sub>BG</sub> to B3<sub>BG</sub> models and B2<sub>BG</sub> to B4<sub>BG</sub> models (**Figure 2a**  
308 and **b**). Indeed, regardless of the used oil, the  $\alpha$ -helix amount increased significantly from 2.7  
309 to 7.1 %, while the  $\beta$ -turn decrease varied in the 10.6 - 14.9 % range (**Figure 2a**). For unordered  
310 structure amount, **Fig. 2a** showed that B3(MO) and B3(SO) contained the highest level,  
311 whereas B3(PO) and B3(RO) represented the lowest amount. Regarding  $\beta$ -sheet structure, the  
312 transition of B1<sub>BG</sub> to B3<sub>BG</sub> models was accompanied by an increase of its variation rate except  
313 for B3(MO).

314 Otherwise, when considering all variation ratios of B4 models on the basis of B2<sub>BG</sub> (**Figure**  
315 **2b**), the  $\alpha$ -helix amount decreased significantly for two vegetal oils with a rate varying from  
316 0.5 % for B4(PO)<sub>BG</sub> to 21.1 % for B4(RO)<sub>BG</sub>. However, the rate of variation increase in  $\beta$ -turn  
317 ranged from 0.8 % for B4(PO)<sub>BG</sub> to 10.1 % B4(MO)<sub>BG</sub>. This difference could be explained by  
318 the fatty acid structure of the vegetable oil. Indeed, fat rich in saturated fatty acids such palmitic  
319 acid (45 % for PO versus 4.6 % for RO) is dispersed in fine droplets in the aqueous phase,  
320 assuring the foaming and emulsion properties, increasing the hydrophobicity of unfolded  
321 proteins, and thus causing the apparition of the  $\beta$ -sheets structures and the loss of unordered  
322 structure.

323 In this context, Han et al. (2021) studied, recently, the effects of fatty acid saturation degree on  
324 protein conformation. Authors showed that the unsaturated degree increased, decreased the  $\alpha$ -  
325 helix, and increased the  $\beta$ -sheet and  $\beta$ -turn levels. Indeed, the  $\alpha$ -helix content was equal to 66.80  
326 % for oleic acid, less than linolenic acid (59.95 %). In addition, the  $\beta$ -turn increased from 13.35

327 % (for oleic acid) to 14.34 % (for linolenic acid). These findings are in agreement with our  
328 results presented in **Fig 2a**.

329 From a mechanistic point of view, the conformation change was ascribed to the re-arrangement  
330 and the formation of an orderly protein backbone during the adsorption at oil/water interfaces.  
331 According to Han et al. (2021), the conformational re-arrangement depends on the transfer of  
332 hydrophobic residues to the oil phase that is influenced by the polarity of the oil phase. The  
333 increase of  $\beta$ -turn content was due to the interaction by hydrophobic groups and disulfide bonds.  
334 The  $\alpha$ -helix was found to facilitate steric repulsion in the interfacial protein layer to avoid  
335 coalescence and flocculation. Thus, fatty acids with higher unsaturation degree induced protein  
336 unfolding, conformational re-arrangement and crosslink to change the emulsification stability.  
337 These findings are in coherence with the study that explored the effect of oil pomaces on the  
338 secondary structures of gluten in a dough model (Rumińska et al., 2020). Indeed, the authors  
339 showed that the  $\beta$ -sheet content increased significantly with the addition of 15 and 20 % oil in  
340 gluten dough in comparison with a control sample.

341 These results indicate that the  $\beta$ -sheet structure is favored by the high content of saturated fatty  
342 acids. It could be also explained by the different behavior of the dispersion of the fat phase and  
343 the crystalline form of triglycerides. Indeed, the co-existence of fat droplets and batter  
344 ingredients changes the nucleation mechanism of the system. So, for solid fats, the  
345 crystallization of triglycerides is often described by a homogeneous nucleation mechanism  
346 contrarily to the heterogeneous nucleation mechanism reported for fat in the continued phase,  
347 allowing the generation of an aqueous phase and increased the availability of water to be  
348 absorbed by starch and proteins and thus favoring the  $\beta$  sheet structure.

349 **3.3.Impact of gelatinization and ingredient interactions on the secondary structure of**  
350 **proteins in slurry and batter models**

351 The gelatinization (heat treatment from 25 to 95 °C) induced significant changes ( $p < 0.05$ )  
352 in the secondary structure of the protein of all slurry and batter systems in both the Amide I and  
353 Amide III regions (**Table 1c** and **d**). For a better understanding of gelatinization impact on the  
354 secondary structure of proteins, the variation rate of each structure was calculated by  
355 considering the formulation BG as the reference. Regarding slurries, the gelatinization  
356 decreased the  $\beta$ -sheet for both S1<sub>AG/BG</sub> (1.4 %) and S2<sub>AG/B</sub> (3.4%) (**Figure 2c**). Similarly, the  
357 unordered content diminished by 7.4 % and 6.5 % for S1<sub>AG/BG</sub>, and S2<sub>AG/BG</sub> respectively, while  
358 the  $\beta$ -turn structure showed an opposed trend with an increasing variation rate of 3.9 % and  
359 27.8 % for S1<sub>AG/BG</sub>, and S2<sub>AG/BG</sub> respectively. Surprisingly for  $\alpha$ -helix structure, different  
360 tendency was observed as a function of the studied system. For instance, the  $\alpha$ -helix structure  
361 content increased strongly for S1<sub>AG/BG</sub> (15.6 %) and slightly for B1<sub>AG/BG</sub> (2.3 %), while it  
362 decreased significantly for S2<sub>AG/BG</sub> (18.3 %) and B2<sub>AG/BG</sub> (13.3 %) (**Figure 2c**).

363 As expected, all the secondary structure contents in batters followed the same variations  
364 observed for slurries (**Figure 2c**). For instance, the gelatinization reduced the amount of  $\beta$ -sheet  
365 structure for B1<sub>AG/BG</sub> (4.9 %) and B2<sub>AG/BG</sub> (7.1 %) as well as the unordered structure (reduction  
366 by 8.2 % and 9.9 % for both B1<sub>AG/BG</sub> and B2<sub>AG/BG</sub>, respectively) at the expense of the increase  
367 of the  $\beta$ -turn structure, which augmented significantly for both B1<sub>AG/BG</sub> (19.6 %) and B2<sub>AG/BG</sub>  
368 (44.6 %), confirming the diminution of  $\beta$ -sheet structure. The same tendency was observed for  
369 slurries. These findings are in agreement with those of Zhongjiang, Yang, Lianzhou, Baokun,  
370 and Linyi (2014), who reported an increase in the percentage of  $\alpha$ -helix structure (observed  
371 with S1<sub>AG/BG</sub> and B1<sub>AG/BG</sub> in our study) and a reduction of the  $\beta$ -sheet structure following heat  
372 treatments (70, 80 and 90 °C for 20 min) of soybean protein isolate; attributed to the partial loss  
373 of  $\beta$ -sheet structure to a self-reassembly from  $\beta$ -sheet in  $\alpha$ -helix and  $\beta$ -turn forms.

374 Zhongjiang et al (2014) suggested that  $\beta$ -conglycinin was denaturated and gradually formed  
375 aggregation, which increased the  $\alpha$ -helix structure but reduced the  $\beta$ -sheet structure. The

376 increased antiparallel  $\beta$ -sheet structure of soy protein heating at a longer period was reported to  
377 be associated with aggregate formed by  $\alpha'$  and  $\alpha$ -7S subunits. Thus, the authors reported that  
378 the involvement of  $\beta$ -sheets in the secondary structure of protein aggregates might be attributed  
379 to the relatively large surface areas for ordered hydrogen bonding and the unfolding of any  
380 higher-ordered structures such as antiparallel  $\beta$ -strands. A recent study on gluten reported an  
381 increase by 27.21 % and 36.61 % for  $\alpha$ -helix and  $\beta$ -sheet at 65 °C followed by 27.21 % and  
382 36.61 % content decrease at 95 °C, respectively (Luo et al., 2016). This finding was interpreted  
383 to the formation of a range of new  $\beta$ -sheet structures together with a shift to weaker hydrogen-  
384 bonded from  $\beta$ -Turn and antiparallel  $\beta$ -sheet structures. From a mechanistic point of view, the  
385 protein degradation of sulfhydryl groups to the disulfide structure strengthens the protein-  
386 protein interactions (Bruun, 2006).

387 To better understand the impact of gelatinization on batter models containing vegetable  
388 fat in comparison with their reference formulations BG (B4(PO)<sub>BG</sub>, B4(RO)<sub>BG</sub>, B4(SO)<sub>BG</sub>,  
389 B4(MO)<sub>BG</sub>), it is more pertinent to calculate the variation rate of discrepancy between  
390 secondary structures amount of B4(PO)<sub>BG</sub> and B4(PO)<sub>AG</sub>, B4(RO)<sub>BG</sub> and B4(RO)<sub>AG</sub>, B4(SO)<sub>BG</sub>  
391 and B4(SO)<sub>AG</sub>, and B4(MO)<sub>BG</sub> and B4(MO)<sub>AG</sub>.

392 Indeed, as shown in **Figure 2d** and regardless of the different structure of fat in the formulation,  
393 the gelatinization decreased the unordered structures (0.2 – 18.5 %) and  $\alpha$ -helix (8.8 - 53.6 %),  
394 while it increased the  $\beta$ -turn (9.7 – 45.5 %) of B4<sub>AG</sub> systems in comparison to B4<sub>BG</sub>. However,  
395 fluctuations as a function of the used oil were found for the  $\beta$ -sheet. For instance, the  $\beta$ -sheet  
396 content increased for both B4(PO)<sub>AG/BG</sub> (3.5 %) and B4(SO)<sub>AG/BG</sub> (3.6 %), while it decreased  
397 for both B4(RO)<sub>AG/BG</sub> (3.5 %) and B4(MO)<sub>AG/BG</sub> (1.6 %). This finding could be explained by  
398 the denaturation of unfolded proteins promoted by the high coefficient of thermal conductivity  
399 of fats that act as a very good heat transmitting agent during gelatinization (Stauffer, 2005).

400           Regarding the Amide III region (**Table 3d**), the variation ranges of secondary structures  
401 were 27.4 – 31.9 % for the  $\beta$ -turn and 22.7 – 26.4 % for the unordered structures. These amounts  
402 were quite similar to those obtained BG (**Table 3b**) in the Amide I region. Indeed, regardless  
403 of the formulation, the protein secondary structure was found to vary between 29.2 and 31 %  
404 for the  $\beta$ -turn, and 23 and 26.1 % for the unordered structures. This result agrees with the  
405 findings in the Amide I region and would confirm that  $\beta$ -turn and the unordered structures were  
406 not very sensitive to the heat treatment.

407           Interestingly, the  $\beta$ -sheet and the  $\alpha$ -helix revealed a greater variation in the Amide III  
408 region following the gelatinization as illustrated in **Figure 2e**, showing a predominant decrease  
409 of the  $\beta$ -sheet structure AG. For instance, for all slurry and batter systems, a reduction average  
410 of 20 % was observed (**Figure 2e**). An opposite trend was found for the  $\alpha$ -helix structure  
411 (**Figure 2f**), where the gelatinization has almost doubled and triplicated its amount. The greatest  
412 increase was observed for the B3(PO) since the variation rate was around 220 %.

413           The novelty of the present paper is based on the understanding of protein secondary  
414 structures changes under gelatinization using different oils in complex matrix (pound cakes)  
415 and the use of MIR spectroscopy for determining their levels. The presented methods and the  
416 obtained results could be deployed in food industry in two ways. Firstly, our findings would  
417 contribute in the improvement of the nutritional values, and thus the gelatinization and  
418 formulation conditions. Secondary, the use of MIR spectroscopy would contribute to the recent  
419 development of hardware (e.g. image techniques, optical sensors, handled instrumentation) in  
420 vibrational spectroscopy methods including MIR spectroscopy and to some extent in the  
421 development of analysis of hyperspectral images for determining the quality of food products  
422 on the basis of the relationships between protein secondary structure and nutrition /  
423 functionality properties.

424 In fact, the review of literature showed that the digestibility of proteins depends tightly on their  
425 molecular structure conformation (Peng et al., 2014). For instance, Qin et al., (2014) proved a  
426 positive correlation between the intestinal absorption of proteins and the percentage of their  $\beta$ -  
427 sheet structures, where higher percentage was assigned with a good digestibility in the small  
428 intestine. This feature was attributed to the large number of hydrogen bonds in  $\beta$ -sheets that can  
429 hinder protease activity. They also confirmed that the nutritional value of proteins feed differed  
430 according to  $\alpha$ -helix-to- $\beta$ -sheet ratio. Previous studies have also reported that this ratio is a good  
431 predictor of nutritional value or digestibility of proteins feed (Theodoridou and Yu, 2017).  
432 Based on these literature findings, it could be concluded that the gelatinization as well as the  
433 use of rapeseed oil would improve the digestibility of cereal products, since they increase the  
434 amount of ordered structure.

435 In another approach, the identification of secondary structure of proteins in presence of  
436 different ingredients, as stated in the present paper, is an important feature in improving the  
437 stability of food matrix. Indeed, the amount of  $\beta$ -sheet and  $\beta$ -turn could affect the techno-  
438 functional properties of proteins such as their emulsion, foaming, gelation, solubility,  
439 rheological, viscosity and water-binding properties. In this context, the increase of  $\alpha$ -helix-to-  
440  $\beta$ -sheet ratio are known to improve the aggregation of proteins and attain enhanced  
441 emulsification, gelation and foaming functional properties. So, the production of stable  
442 emulsion and foam systems such as ice cream, salad dressing, and yogurt would be fully  
443 controlled by the identification of protein structures (Lafarga et al., 2020). Thus, establishing a  
444 relationship between the molecular structure characteristics of proteins is a good indicator for  
445 industries to confirm their nutritional value and their techno-functional properties.

446 Regarding developments in hardware, software and sensing technologies in vibrational  
447 spectroscopy, they are supposed to contribute in the improvement of the existing capabilities  
448 and incorporating new processing technologies (e.g., real time monitoring of processes and

449 storage conditions throughout food production). According to Cozzolino (2021), the  
450 incorporation of digital and technological innovations is necessary to increase the information  
451 gathered in a single process in food industry. Indeed, knowledge and understanding of food  
452 properties and the complexity of food (e.g., composition, functionality) in the context of the  
453 food matrices and the property-relationships needed to develop sensors (Blecker & al., 2012;  
454 Karoui et al; 2008). Some authors have reported recently the importance of vibrational  
455 spectroscopy such as MIR spectroscopy in the process analytical technologies for collecting  
456 chemical information during the processing of foods (e.g., spatial and temporal information)  
457 (Eifert, Eisen, Maiwald, & Herwig, 2020; Herwig, 2020). The implementation of MIR  
458 spectroscopy into processing has been possible due to the availability of a wide range and type  
459 of sensors that can provide with fast, reliable and robust analytical data.

460

#### 461 **4. Conclusion**

462 The MIR spectroscopy demonstrated its ability to explore the conformational changes of  
463 starch and secondary structure of proteins in slurry and batter models of pound cakes systems  
464 as a function of the gelatinization and the different fat structure and the use of thickening agent.  
465 In the Amide I region, the obtained results suggest that  $\beta$ -sheet and  $\beta$ -turn are dramatically  
466 modified by the addition of batter ingredients (fat, sugar, salt and whole egg) due to the  
467 competition towards the water. However, the unordered and the  $\alpha$ -helix structures are the most  
468 affected by the addition of the thickening agent AG. Additionally, gelatinization was found to  
469 reduce the hydrogen-bonding capacity through the reduction of water availability for  
470 ingredients and thus increasing  $\beta$ -sheet at the expense of  $\beta$ -turn. The findings in the Amide III  
471 region suggested that this region is still very promising to estimate protein secondary structure  
472 content. In addition, the understanding of proteins secondary structures changes will strengthen

473 the current knowledge on their nutritional values and their emulsification and foam stabilization  
474 properties.

475 Amylose and amylopectin structures depend also on ingredient interactions and gelatinization.  
476 The different ratios showed that the addition of ingredients was accompanied by system  
477 stabilization and structuration. Moreover, the enhancements of baked product quality involve  
478 a deep knowledge of the morphology of fat crystals side by side to the understanding of  
479 interactions between different ingredients at the interfaces.

480 The present work showed a real potential of MIR spectroscopy for protein secondary structure  
481 evaluation, which may contribute to tackle some challenges such as the reluctance by the food  
482 industry to integrate this type of technology during the routine analysis control of foods and  
483 ingredients and foods, or to monitor the food manufacturing process.

484

485 **Acknowledgments:**

486 This work has been carried out in the framework of ALIBIOTECH project, which is financed  
487 by the European Union, the French State and the French Region of Hauts-de-France. The  
488 authors gratefully acknowledge the financial support from the Major Domain of Interest (DIM)  
489 "Eco-Energy Efficiency" of Artois University. Mrs. Z. Nhouchi is grateful to the Artois  
490 University for the financial support of her Ph.D.

491

492 **References**

- 493 Ait-Ameur, L. (2006). *Evolution de la qualité nutritionnelle des protéines de biscuits modèles*  
 494 *au cours de la cuisson au travers d'indicateurs de la réaction de Maillard: Intérêt de la*  
 495 *fluorescence frontale*. Institut National Agronomique, Paris, France.
- 496 Baltacıoğlu, H., Bayındırlı, A., Severcan, M., & Severcan, F. (2015). Effect of thermal  
 497 treatment on secondary structure and conformational change of mushroom polyphenol  
 498 oxidase (PPO) as food quality related enzyme: A FTIR study. *Food Chemistry*, 187,  
 499 263-269. doi: <https://doi.org/10.1016/j.foodchem.2015.04.097>
- 500 Beck, S. M., Knoerzer, K., & Arcot, J. (2017). Effect of low moisture extrusion on a pea protein  
 501 isolate's expansion, solubility, molecular weight distribution and secondary structure as  
 502 determined by Fourier Transform Infrared Spectroscopy (FTIR). *Journal of Food*  
 503 *Engineering*, 214, 166-174. doi: <https://doi.org/10.1016/j.jfoodeng.2017.06.037>
- 504 Blecker, C., Jiwan, J-M.H., & Karoui, R. (2012) Effect of heat treatment of rennet skim milk  
 505 induced coagulation on the rheological properties and molecular structure determined  
 506 by synchronous fluorescence spectroscopy and turbiscan. *Food Chemistry*, 35, 1809-  
 507 1817.
- 508 Bock, J. E., & Damodaran, S. (2013). Bran-induced changes in water structure and gluten  
 509 conformation in model gluten dough studied by Fourier transform infrared  
 510 spectroscopy. *Food Hydrocolloids*, 31(2), 146-155. doi:  
 511 <https://doi.org/10.1016/j.foodhyd.2012.10.014>
- 512 Bruun, S. W. (2006). *Spectroscopic detection of macromolecular interactions focusing on*  
 513 *protein-protein interactions in food*. Technical University of Denmark.
- 514 Cai, S., & Singh, B. (1999). Identification of  $\beta$ -turn and random coil amide III infrared bands  
 515 for secondary structure estimation of proteins. *Biophysical Chemistry*, 80(1), 7-20. doi:  
 516 [https://doi.org/10.1016/S0301-4622\(99\)00060-5](https://doi.org/10.1016/S0301-4622(99)00060-5)
- 517 Campbell, L., Euston, S. R., & Ahmed, M. A. (2016). Effect of addition of thermally modified  
 518 cowpea protein on sensory acceptability and textural properties of wheat bread and  
 519 sponge cake. *Food Chemistry*, 194, 1230-1237. doi: 1  
 520 <https://doi.org/10.1016/j.foodchem.2015.09.002>
- 521 Campbell, L., Raikos, V., & Euston, S. R. (2003). Modification of functional properties of egg-  
 522 white proteins *Nahrung Weinheim*, 47(6), 369-376. doi:  
 523 <https://doi.org/10.1002/food.200390084>
- 524 Copeland, L., Li, C., Niu, Q., & Wang, S. (2015). Starch retrogradation: a comprehensive  
 525 review. *Comprehensive Reviews in Food Science and Food Safety*(5), 568-573. doi:  
 526 <https://doi.org/10.1111/1541-4337.12143>
- 527 Cozzolino, D. (2021). From consumers' science to food functionality – Challenges and  
 528 opportunities for vibrational spectroscopy. *Advances in Food and Nutrition Research*,  
 529 97(2), 119 – 146. doi: 10.1016/bs.afnr.2021.03.002
- 530 Devi, A., & Khatkar, B. S. (2018). Effects of fatty acids composition and microstructure  
 531 properties of fats and oils on textural properties of dough and cookie quality. *J Food Sci*  
 532 *Technol*, 55(1), 321-330. doi: <https://doi.org/10.1007/s13197-017-2942-8>
- 533 Duan, X., Li, M., Shao, J., Chen, H., Xu, X., Jin, Z., & Liu, X. (2018). Effect of oxidative  
 534 modification on structural and foaming properties of egg white protein. *Food*  
 535 *Hydrocolloids*, 75, 223-228. doi: <https://doi.org/10.1016/j.foodhyd.2017.08.008>
- 536 Eifert, T., Eisen, K., Maiwald, M., & Herwig, C. (2020). Current and future requirements to  
 537 industrial analytical infrastructure-Part 2: Smart sensors. *Analytical and Bioanalytical*  
 538 *Chemistry*, 412, 2037–2045. doi: 10.1007/s00216-020-02421-1
- 539 Fevzioglu, M., Ozturk, O. K., Hamaker, B. R., & Campanella, O. H. (2020). Quantitative  
 540 approach to study secondary structure of proteins by FT-IR spectroscopy, using a model

541 wheat gluten system. *International Journal of Biological Macromolecules*, 164, 2753-  
542 2760. doi: <https://doi.org/10.1016/j.ijbiomac.2020.07.299>

543 Flores-Morales, A., Jiménez-Estrada, M., & Mora-Escobedo, R. (2012). Determination of the  
544 structural changes by FT-IR, Raman, and CP/MAS <sup>13</sup>C NMR spectroscopy on  
545 retrograded starch of maize tortillas. *Carbohydrate Polymers*, 87(1), 61-68. doi:  
546 <http://dx.doi.org/10.1016/j.carbpol.2011.07.011>

547 Georget, D. M., & Belton, P. S. (2006). Effects of temperature and water content on the  
548 secondary structure of wheat gluten studied by FTIR spectroscopy. *Biomacromolecules*,  
549 7(2), 469-475. doi: <https://doi.org/10.1021/bm050667j>

550 Gómez, A. V., Ferrer, E. G., Añón, M. C., & Puppo, M. C. (2013). Changes in secondary  
551 structure of gluten proteins due to emulsifiers. *Journal of Molecular Structure*, 1033,  
552 51-58. doi: <https://doi.org/10.1016/j.molstruc.2012.08.031>

553 Guraya, H. S., Kadan, R., & Champagne, E. T. (1997). Effect of rice starch–lipid complexes on  
554 in vitro digestibility, complexing index, and viscosity. *Cereal Chemistry*, 74(5), 561–  
555 565. doi: <https://doi.org/10.1094/CCHEM.1997.74.5.561>

556 Han, Z., Xu, S., Sun, J., Yue, X., Wu, Z., & Shao, J. H. (2021). Effects of fatty acid saturation  
557 degree on salt-soluble pork protein conformation and interfacial adsorption  
558 characteristics at the oil/water interface. *Food Hydrocolloids*, 113, 106472. doi:  
559 <https://doi.org/10.1016/j.foodhyd.2020.106472>

560 Hesso, N., Loisel, C., Chevallier, S., Le-Bail, A., Queveau, D., Pontoire, B., & Le-Bail, P.  
561 (2015). Monitoring cake baking by studying different ingredient interactions: from a  
562 model system to a real system. *Food Hydrocolloids*, 51, 7-15. doi:  
563 <http://dx.doi.org/10.1016/j.foodhyd.2015.04.013>

564 Hesso, N., Marti, A., Le-Bail, P., Loisel, C., Chevallier, S., Le-Bail, A., & Seetharaman, K.  
565 (2015). Conformational changes of polymers in model batter systems. *Food*  
566 *Hydrocolloids*, 51, 101-107. doi: <http://dx.doi.org/10.1016/j.foodhyd.2015.05.010>

567 Jacobsen, C., & Hu, M. (2016). *Oxidative Stability and Shelf Life of Foods Containing Oils and*  
568 *Fats*. San Diego, CA: Academic Press and AOCS Press.

569 Herwig, C. (2020). Applied basic science in process analytics and control technology.  
570 *Analytical and Bioanalytical Chemistry*.412(4), 2025–2026. doi.org/10.1007/s00216-  
571 020-02465-3

572 Karoui, R., Nicolaï, B., & De Baerdemaeker, J. (2008) Monitoring the egg-freshness during  
573 storage under modified atmosphere by fluorescence spectroscopy. *Food and Bioprocess*  
574 *Technology*, 1, 346-356

575 Lafarga, T., Álvarez, C., Villaró, S., Bobo., G and Aguiló-Aguayo, I. Potential of pulse-derived  
576 proteins for developing novel novel vegan edible foams and emulsions, *Int. J. Food Sci.*  
577 *Technol.*, 2020, 55, 475

578 Lamacchia, C., Landriscina, L., & D'Agello, P. (2016). Changes in wheat kernel proteins  
579 induced by microwave treatment. *Food Chemistry*, 197, 634-640. doi:  
580 <https://doi.org/10.1016/j.foodchem.2015.11.016>

581 Luo, Y., Li, M., Zhu, K. X., Guo, X. N., Peng, W., & Zhou, H. M. (2016). Heat-induced  
582 interaction between egg white protein and wheat gluten. *Food Chemistry*, 197, 699-708.  
583 doi: <https://doi.org/10.1016/j.foodchem.2015.09.088>

584 Nawrocka, A., Miś, A., & Niewiadomski, Z. (2017). Dehydration of gluten matrix as a result  
585 of dietary fibre addition – A study on model flour with application of FT-IR  
586 spectroscopy. *Journal of Cereal Science*, 74, 86-94. doi:  
587 <https://doi.org/10.1016/j.jcs.2017.02.001>

588 Nhouchi, Z., & Karoui, R. (2018). Application of Fourier-transform mid infrared spectroscopy  
589 for the monitoring of pound cakes quality during storage. *Food Chemistry*, 252, 327-  
590 334. doi: <https://doi.org/10.1016/j.foodchem.2018.01.122>

- 591 Ortiz, D. E. (2004). Cakes, Pastries, Muffins, and bagels. In C. Wrigley (Ed.), *Encyclopedia of*  
592 *Grain Science* (pp. 134-140). Oxford: Elsevier.
- 593 Peng, Q. H., N. A. Khan, Z. Wang, and P. Q. Yu. 2014. Relationship of feeds protein structural  
594 makeup in common Prairie feeds with protein solubility, in situ ruminal degradation and  
595 intestinal digestibility. *Anim. Feed Sci. Technol.* 194:58-70
- 596 Qin, G. X., Z. W. Sun, G. H. Long, T. Wang, and M. M. Bai. 2014. The physicochemical  
597 property of feedstuff proteins and its effects on the nutritional value. *Chin. J. Anim.*  
598 *Nutr.* 26:1-7
- 599 Rumińska, W., Szymańska-Chargot, M., Wiącek, D., Sobota, A., Markiewicz, K. H.,  
600 Wilczewska, A. Z., Nawrocka, A. (2020). FT-Raman and FT-IR studies of the gluten  
601 structure as a result of model dough supplementation with chosen oil pomaces. *Journal*  
602 *of Cereal Science*, 93, 102961. doi: <https://doi.org/10.1016/j.jcs.2020.102961>
- 603 Seabourn, B. W., Chung, O. K., Seib, P. A., & Mathewson, P. R. (2008). Determination of  
604 Secondary Structural Changes in Gluten Proteins during Mixing Using Fourier  
605 Transform Horizontal Attenuated Total Reflectance Spectroscopy. *Journal of*  
606 *Agricultural and Food Chemistry*, 56(11), 4236-4243. doi:  
607 <https://doi.org/10.1021/jf703569b>
- 608 Secundo, F., & Guerrieri, N. (2005). ATR-FT/IR study on the interactions between gliadins and  
609 dextrin and their effects on protein secondary structure. *Journal of agricultural and food*  
610 *chemistry*, 53, 1757-1764. doi: <https://doi.org/10.1021/jf049061x>
- 611 Shehzad, A. (2010). *Rôle du pétrissage de farine de blé sur les propriétés rhéologiques de la*  
612 *pâte et la texture du pain*. Université de Nantes, Nantes, France. (225)
- 613 Singh, B. R., DeOliveira, D. B., Fu, F. N., & Fuller, M. P. (1993). Fourier transform infrared  
614 15analysis of amide III bands of proteins for the secondary structure estimation.  
615 *Proceedings of Biomolecular Spectroscopy volume, 1890(13)*, 47-55. doi:  
616 <https://doi.org/10.1117/12.145242>
- 617 Sivam, A. S., Sun-Waterhouse, D., Perera, C. O., & Waterhouse, G. I. N. (2013). Application  
618 of FT-IR and Raman spectroscopy for the study of biopolymers in breads fortified with  
619 fibre and polyphenols. *Food Research International*, 50(2), 574-585. doi:  
620 <http://dx.doi.org/10.1016/j.foodres.2011.03.039>
- 621 Stauffer, C. E. (2005). Fats and oils in bakery products *Bailey's Industrial Oil and Fat Products*:  
622 John Wiley & Sons, Inc.
- 623 Theodoridou, K. and P. Yu. 2017. Application potential of ATRFT/IR molecular spectroscopy  
624 in animal nutrition: Reveal protein molecular structures of canola meal and presscake,  
625 as affected by heat processing methods, in relationship with their protein digestive  
626 behavior and utilization for dairy cattle. *J. Agric. Food Chem.* 61:5449-5458
- 627 Ulrichs, T., Drotleff, A. M., & Ternes, W. (2015). Determination of heat-induced changes in  
628 the protein secondary structure of reconstituted livetins (water-soluble proteins from  
629 hen's egg yolk) by FTIR. *Food Chemistry*, 172, 909-920. doi:  
630 <https://doi.org/10.1016/j.foodchem.2014.09.128>
- 631 Warren, F. J., Perston, B., Royall, P., Butterworth, P., & Ellis, P. (2013). Infrared spectroscopy  
632 with heated attenuated total internal reflectance enabling precise measurement of  
633 thermally induced transitions in complex biological polymers. *Analytical chemistry*, 85,  
634 3999-4006. doi: <https://doi.org/10.1021/ac303552s>.
- 635 Widjanarko, S. B., Nugroho, A., & Estiasih, T. (2011). Functional interaction components of  
636 protein isolates and glucomannan in food bars by FTIR and SEM studies. *African*  
637 *Journal of Food Science* 5(1), 12-21.

638 Ye, M. P., Zhou, R., Shi, Y. R., Chen, H. C., & Du, Y. (2017). Effects of heating on the  
639 secondary structure of proteins in milk powders using mid-infrared spectroscopy.  
640 *Journal of Dairy Science*, 100(1), 89-95. doi: <https://doi.org/10.3168/jds.2016-11443>  
641 Zhongjiang, W., Yang, L., Lianzhou, J., Baokun, Q., & Linyi, Z. (2014). Relationship between  
642 secondary structure and surface hydrophobicity of soybean protein isolate subjected to  
643 heat treatment. *Journal of Chemistry*, 10(1), 1-10.  
644 doi:<https://doi.org/10.1155/2014/475389>  
645

646 **List of tables**

647

648 **Table 1:** (a) Recipes of different slurry (S) and batter (B) models formulated with rapeseed oil  
649 (RO), palm oil (PO), sunflower oil (SO) and mixture oil (MO) (b) Absorption frequencies of  
650 proteins secondary structures in both Amide I and amide III regions (Hesso et al., 2015;  
651 Seabourn et al., 2008)

652

653 **Table 2:** Conformational changes of starch determined from absorbance intensity ratios of  
654 slurry and batter models (a) before gelatinization (BG) and (b) after gelatinization (AG)

655

656 **Table 3:** Conformational changes in the secondary structures of proteins for slurry and batter  
657 models before gelatinization (BG) (a, b) and after gelatinization (AG) (c, d) in Amide I region  
658 (a, c) and Amide III region (b, d)

659

660

661 **List of figures**

662

663

664 **Figure 1:** (a) Raw MIR spectra and their corresponding second derivative Savitzky-Golay  
665 spectra recorded on the Amide I region  $1600 - 1700 \text{ cm}^{-1}$  and (b) Amide III region acquired on  
666 (i) flour system S2 before gelatinization (BG) (-.-.-) and after gelatinization (AG) (...); and (ii)  
667 on batter system B2 before gelatinization (BG) (—) and after gelatinization (AG) (---)

668

669 **Figure 2:** Variation of conformational changes of (a, b, c, and d) secondary structure of proteins  
670 and focus on (e)  $\beta$ -sheet and (f)  $\alpha$ -helix in (c, e, and f) slurry and (a, b, c, d, e, and f) batter  
671 models (a, and b) before gelatinization and (c, and d) induced by gelatinization, thickening  
672 agent addition and the botanical origin of fat used in the formulation

673

674

**Table 1a:**

	Abbreviations	Composition of models
SLURRY (S)	S1	Wheat flour + water
	S2	Wheat flour + water + <i>egg yolk</i> + <i>native starch</i>
	S3 (RO, PO, SO, MO)	Wheat flour + water + <b>fat</b>
	S4 (RO, PO, SO, MO)	Wheat flour + water + <i>egg yolk</i> + <i>native starch</i> + <b>fat</b>
BATTER (B)	B1	Wheat flour + water + sugar + liquid whole egg + salt
	B2	Wheat flour + water + sugar + liquid whole egg + salt + <i>egg yolk</i> + <i>native starch</i>
	B3 (RO, PO, SO, MO)	Wheat flour + water + sugar + liquid whole egg + salt + <b>fat</b>
	B4 (RO, PO, SO, MO)	Wheat flour + water + sugar + liquid whole egg + salt + <i>egg yolk</i> + <i>native starch</i> + <b>fat</b>

675

**Egg yolk + native starch = thickening agent**

676

**Four formulations were prepared for models containing fat (S3, S4, B3, and B4) in function of the 4 vegetable oils selected (RO, PO, SO, MO)**

677

678

679

**Table 1b:**

	Wheat flour (% wb of flour)	Native starch (% wb of flour)	Egg yolk (% wb of flour)	Fat (% wb of flour)	Liquid whole egg (% wb of flour)	Crystal sugar (% wb of flour)	Salt (% wb of flour)
S1	100	0	0	0	0	0	0
S2	100	0.5	7.5	0	0	0	0
S3	100	0	0	83.7	0	0	0
S4	100	0.5	7.5	75.6	0	0	0
B1	100	0	0	0	100	100	1.6
B2	100	0.5	7.5	0	100	100	1.6
B3	100	0	0	83.7	100	100	1.6
B4	100	0.5	7.5	75.6	100	100	1.6

680

681

**Table 1c:**

<b>Secondary structures of proteins</b>	<b>Amide I region</b>	<b>Amide III region</b>
$\beta$ -sheet	1620 - 1641 $\text{cm}^{-1}$	1220 - 1245 $\text{cm}^{-1}$
random coil structures (unordered)	1641 - 1650 $\text{cm}^{-1}$	1245 - 1270 $\text{cm}^{-1}$
$\alpha$ -helix	1650 - 1660 $\text{cm}^{-1}$	1295 - 1330 $\text{cm}^{-1}$
$\beta$ -turns	1660 - 1684 $\text{cm}^{-1}$	1270 - 1295 $\text{cm}^{-1}$

682

683

**Table 2a:**

	R <sub>1</sub> (1022 cm <sup>-1</sup> / 995 cm <sup>-1</sup> )	R <sub>2</sub> (1047 cm <sup>-1</sup> / 1022 cm <sup>-1</sup> )	R <sub>3</sub> (1047 cm <sup>-1</sup> / 1035 cm <sup>-1</sup> )
S1 <sub>BG</sub>	1.001 <sup>c</sup> ± 0.008	0.860 <sup>f</sup> ± 0.008	0.951 <sup>f</sup> ± 0.003
S2 <sub>BG</sub>	0.996 <sup>d</sup> ± 0.003	0.900 <sup>e</sup> ± 0.006	0.971 <sup>e</sup> ± 0.002
S3(RO) <sub>BG</sub>	1.022 <sup>bc</sup> ± 0.005	0.910 <sup>e</sup> ± 0.006	0.981 <sup>de</sup> ± 0.002
S3(PO) <sub>BG</sub>	1.082 <sup>ab</sup> ± 0.002	0.870 <sup>ef</sup> ± 0.001	0.950 <sup>ef</sup> ± 0.001
S3(SO) <sub>BG</sub>	1.091 <sup>ab</sup> ± 0.001	0.901 <sup>e</sup> ± 0.001	0.970 <sup>e</sup> ± 0.001
S3(MO) <sub>BG</sub>	1.100 <sup>a</sup> ± 0.001	0.872 <sup>ef</sup> ± 0.001	0.950 <sup>ef</sup> ± 0.001
S4(RO) <sub>BG</sub>	1.030 <sup>b</sup> ± 0.002	0.980 <sup>de</sup> ± 0.002	1.011 <sup>d</sup> ± 0.001
S4(PO) <sub>BG</sub>	1.040 <sup>b</sup> ± 0.002	0.980 <sup>de</sup> ± 0.010	1.001 <sup>d</sup> ± 0.003
S4(SO) <sub>BG</sub>	1.091 <sup>ab</sup> ± 0.001	0.941 <sup>def</sup> ± 0.002	0.990 <sup>de</sup> ± 0.000
S4(MO) <sub>BG</sub>	1.090 <sup>ab</sup> ± 0.001	0.893 <sup>ef</sup> ± 0.002	0.960 ± 0.001
B1 <sub>BG</sub>	0.871 <sup>ef</sup> ± 0.003	1.121 <sup>bc</sup> ± 0.01	1.111 <sup>bc</sup> ± 0.004
B2 <sub>BG</sub>	0.891 <sup>e</sup> ± 0.001	1.100 <sup>d</sup> ± 0.011	1.101 <sup>bc</sup> ± 0.005
B3(RO) <sub>BG</sub>	0.881 <sup>ef</sup> ± 0.004	1.120 <sup>c</sup> ± 0.031	1.110 <sup>c</sup> ± 0.015
B3(PO) <sub>BG</sub>	0.890 <sup>ef</sup> ± 0.003	1.121 <sup>c</sup> ± 0.013	1.110 <sup>b</sup> ± 0.005
B3(SO) <sub>BG</sub>	0.860 <sup>f</sup> ± 0.003	1.131 <sup>b</sup> ± 0.011	1.110 <sup>bc</sup> ± 0.004
B3(MO) <sub>BG</sub>	0.860 <sup>f</sup> ± 0.001	1.150 <sup>a</sup> ± 0.002	1.121 <sup>a</sup> ± 0.001
B4(RO) <sub>BG</sub>	0.850 <sup>f</sup> ± 0.003	1.150 <sup>ab</sup> ± 0.005	1.110 <sup>b</sup> ± 0.003
B4(PO) <sub>BG</sub>	0.860 <sup>f</sup> ± 0.001	1.140 <sup>ab</sup> ± 0.002	1.110 <sup>b</sup> ± 0.002
B4(SO) <sub>BG</sub>	0.881 <sup>ef</sup> ± 0.004	1.110 <sup>c</sup> ± 0.021	1.100 <sup>c</sup> ± 0.008
B4(MO) <sub>BG</sub>	0.881 <sup>ef</sup> ± 0.001	1.131 <sup>bc</sup> ± 0.026	1.110 <sup>c</sup> ± 0.010

685 Different small letters (a, b, c, d, e, and f) represent statistical differences between different storage days ( $p < 0.05$ ); BG: before gelatinization;  
686 RO, PO, SO and MO: rapeseed oil, palm oil sunflower oil and mixture oil (60 % of sunflower oil), respectively.

**Table 2b:**

	R <sub>1</sub> (1022 cm <sup>-1</sup> / 995 cm <sup>-1</sup> )	R <sub>2</sub> (1047 cm <sup>-1</sup> / 1022 cm <sup>-1</sup> )	R <sub>3</sub> (1047 cm <sup>-1</sup> / 1035 cm <sup>-1</sup> )
S1 <sub>AG</sub>	1.190 <sup>a</sup> ± 0.002	0.871 <sup>f</sup> ± 0.001	0.931 <sup>e</sup> ± 0.001
S2 <sub>AG</sub>	1.210 <sup>a</sup> ± 0.002	0.951 <sup>d</sup> ± 0.002	0.972 <sup>c</sup> ± 0.002
S3(RO) <sub>AG</sub>	1.061 <sup>b</sup> ± 0.001	0.911 <sup>e</sup> ± 0.001	0.951 <sup>d</sup> ± 0.001
S3(PO) <sub>AG</sub>	1.056 <sup>b</sup> ± 0.002	0.921 <sup>e</sup> ± 0.001	0.960 <sup>cd</sup> ± 0.001
S3(SO) <sub>AG</sub>	1.047 <sup>b</sup> ± 0.002	0.941 <sup>d</sup> ± 0.001	0.961 <sup>cd</sup> ± 0.001
S3(MO) <sub>AG</sub>	0.980 <sup>cd</sup> ± 0.012	0.970 <sup>c</sup> ± 0.007	0.991 <sup>bc</sup> ± 0.005
S4(RO) <sub>AG</sub>	1.071 <sup>b</sup> ± 0.003	0.911 <sup>e</sup> ± 0.001	0.951 <sup>d</sup> ± 0.001
S4(PO) <sub>AG</sub>	1.022 <sup>bc</sup> ± 0.002	0.940 <sup>d</sup> ± 0.002	0.970 <sup>c</sup> ± 0.001
S4(SO) <sub>AG</sub>	1.011 <sup>bc</sup> ± 0.002	0.950 <sup>d</sup> ± 0.001	0.972 <sup>c</sup> ± 0.002
S4(MO) <sub>AG</sub>	1.041 <sup>b</sup> ± 0.001	0.931 <sup>de</sup> ± 0.001	0.964 <sup>cd</sup> ± 0.001
B1 <sub>AG</sub>	0.941 <sup>d</sup> ± 0.001	1.002 <sup>ab</sup> ± 0.002	1.021 <sup>a</sup> ± 0.001
B2 <sub>AG</sub>	0.941 <sup>d</sup> ± 0.001	1.001 <sup>ab</sup> ± 0.002	1.022 <sup>a</sup> ± 0.001
B3(RO) <sub>AG</sub>	0.950 <sup>d</sup> ± 0.001	0.982 <sup>bc</sup> ± 0.001	1.001 <sup>ab</sup> ± 0.001
B3(PO) <sub>AG</sub>	0.951 <sup>d</sup> ± 0.004	1.001 <sup>b</sup> ± 0.004	1.011 <sup>ab</sup> ± 0.002
B3(SO) <sub>AG</sub>	1.031 <sup>b</sup> ± 0.002	0.932 ± 0.002	0.961 <sup>cd</sup> ± 0.002
B3(MO) <sub>AG</sub>	0.941 <sup>d</sup> ± 0.001	1.011 <sup>a</sup> ± 0.002	1.021 <sup>a</sup> ± 0.002
B4(RO) <sub>AG</sub>	0.981 <sup>c</sup> ± 0.05	0.981 <sup>cd</sup> ± 0.044	0.991 <sup>c</sup> ± 0.033
B4(PO) <sub>AG</sub>	0.950 <sup>d</sup> ± 0.002	1.001 <sup>ab</sup> ± 0.001	1.022 <sup>a</sup> ± 0.001
B4(SO) <sub>AG</sub>	0.971 <sup>c</sup> ± 0.001	0.982 <sup>bc</sup> ± 0.001	0.991 <sup>b</sup> ± 0.001
B4(MO) <sub>AG</sub>	0.961 <sup>c</sup> ± 0.001	0.981 <sup>bc</sup> ± 0.002	1.010 <sup>ab</sup> ± 0.002

688 Different small letters (a, b, c, d, e, and f) represent statistical differences between different storage days ( $p < 0.05$ ); AG: After gelatinization;  
689 RO, PO, SO and MO: rapeseed oil, palm oil sunflower oil and mixture oil (60 % of sunflower oil), respectively.

**Table 3a:**

	$\beta$ -sheets	unordered	$\alpha$ -helix	$\beta$ -turns
Wheat flour	31.6 <sup>i</sup> ± 1.1	15.4 <sup>e</sup> ± 1.0	40.3 <sup>a</sup> ± 0.5	12.7 <sup>hi</sup> ± 0.3
Whole egg	55 <sup>a</sup> ± 0.6	18 <sup>cd</sup> ± 0.3	13.6 <sup>cd</sup> ± 0.9	13.4 <sup>h</sup> ± 0.8
yolk	51.5 <sup>de</sup> ± 1.2	19.4 <sup>bcd</sup> ± 1.0	17.7 <sup>b</sup> ± 0.5	11.4 <sup>hi</sup> ± 0.5
S1 <sub>BG</sub>	51.2 <sup>def</sup> ± 0.0	18.9 <sup>cd</sup> ± 0.0	9.6 <sup>g</sup> ± 0.0	20.2 <sup>a</sup> ± 0.0
S2 <sub>BG</sub>	52.8 <sup>c</sup> ± 0.0	18.5 <sup>cd</sup> ± 0.0	10.9 <sup>efg</sup> ± 0.0	17.9 <sup>cde</sup> ± 0.0
S3(RO) <sub>BG</sub>	50.4 <sup>fgh</sup> ± 0.0	20.5 <sup>cd</sup> ± 0.0	9.9 <sup>fg</sup> ± 0.0	19.1 <sup>ab</sup> ± 0.0
S3(PO) <sub>BG</sub>	<b>54.9<sup>a</sup> ± 0.0</b>	20.2 <sup>bcd</sup> ± 0.0	6.7 <sup>h</sup> ± 0.0	18.2 <sup>cd</sup> ± 0.0
S3(SO) <sub>BG</sub>	51.6 <sup>d</sup> ± 0.0	25 <sup>a</sup> ± 0.1	14.4 <sup>c</sup> ± 0.0	9.1 <sup>i</sup> ± 0.0
S3(MO) <sub>BG</sub>	50.6 <sup>efgh</sup> ± 0.0	23.9 <sup>ab</sup> ± 0.0	13.1 <sup>cd</sup> ± 0.0	12.5 <sup>hi</sup> ± 0.0
S4(RO) <sub>BG</sub>	51.5 <sup>de</sup> ± 0.0	20.1 <sup>bcd</sup> ± 0.0	13.7 <sup>cd</sup> ± 0.0	14.7 <sup>h</sup> ± 0.0
S4(PO) <sub>BG</sub>	<b>53.8<sup>b</sup> ± 0.0</b>	20.4 <sup>bcd</sup> ± 0.0	11.4 <sup>defg</sup> ± 0.0	14.5 <sup>h</sup> ± 0.0
S4(SO) <sub>BG</sub>	49.9 <sup>h</sup> ± 0.0	21.3 <sup>bc</sup> ± 0.1	17.1 <sup>b</sup> ± 0.0	11.6 <sup>hi</sup> ± 0.0
S4(MO) <sub>BG</sub>	51.1 <sup>defg</sup> ± 0.0	19.8 <sup>cd</sup> ± 0.0	12.6 <sup>bcd</sup> ± 0.0	16.6 <sup>def</sup> ± 0.0
B1 <sub>BG</sub>	50.6 <sup>efgh</sup> ± 0.0	18.3 <sup>cd</sup> ± 0.1	12.3 <sup>bcd</sup> ± 0.01	18.8 <sup>bc</sup> ± 0.0
B2 <sub>BG</sub>	51.2 <sup>def</sup> ± 0.0	18.8 <sup>cd</sup> ± 0.0	13.5 <sup>cd</sup> ± 0.1	16.4 <sup>efg</sup> ± 0.0
B3(RO) <sub>BG</sub>	51.9 <sup>cd</sup> ± 0.0	18.7 <sup>cd</sup> ± 0.0	12.7 <sup>bcd</sup> ± 0.0	16.8 <sup>def</sup> ± 0.0
B3(PO) <sub>BG</sub>	<b>52.6<sup>c</sup> ± 0.0</b>	18.2 <sup>cd</sup> ± 0.0	13.1 <sup>cde</sup> ± 0.0	16.0 <sup>fg</sup> ± 0.0
B3(SO) <sub>BG</sub>	51.1 <sup>defg</sup> ± 0.0	19.8 <sup>bcd</sup> ± 0.0	12.7 <sup>cdef</sup> ± 0.0	16.4 <sup>efg</sup> ± 0.0
B3(MO) <sub>BG</sub>	50.2 <sup>gh</sup> ± 0.0	20.9 <sup>bcd</sup> ± 0.0	12.6 <sup>cdef</sup> ± 0.1	16.3 <sup>efg</sup> ± 0.0
B4(RO) <sub>BG</sub>	50.1 <sup>gh</sup> ± 0.0	19.9 <sup>bcd</sup> ± 0.0	13.5 <sup>cd</sup> ± 0.0	16.6 <sup>def</sup> ± 0.0
B4(PO) <sub>BG</sub>	<b>54<sup>ab</sup> ± 0.0</b>	17.9 <sup>c</sup> ± 0.0	10.6 <sup>fg</sup> ± 0.0	17.5 <sup>cdef</sup> ± 0.0
B4(SO) <sub>BG</sub>	48.3 <sup>h</sup> ± 0.0	21.3 <sup>bc</sup> ± 0.0	13 <sup>cdef</sup> ± 0.0	17.4 <sup>cdef</sup> ± 0.0
B4(MO) <sub>BG</sub>	50.6 <sup>gh</sup> ± 0.0	20.0 <sup>bcd</sup> ± 0.0	11.3 <sup>defg</sup> ± 0.0	18.1 <sup>cd</sup> ± 0.1

691 Different small letters (a, b, c, d, e, f, g, h and i) represent statistical differences between different storage days ( $p < 0.05$ ); BG: before  
692 gelatinization; RO, PO, SO and MO: rapeseed oil, palm oil sunflower oil and mixture oil (60 % of sunflower oil), respectively.

**Table 3b:**

	$\beta$ -sheets	unordered	$\alpha$ -helix	$\beta$ -turns
S1 <sub>BG</sub>	37.8 <sup>d</sup> ± 0.0	23.1 <sup>gh</sup> ± 0.0	8.7 <sup>e</sup> ± 0.0	30.4 <sup>b</sup> ± 0.0
S2 <sub>BG</sub>	37.5 <sup>e</sup> ± 0.0	23.2 <sup>g</sup> ± 0.0	9.0 <sup>d</sup> ± 0.0	30.3 <sup>c</sup> ± 0.0
<b>S3(RO)<sub>BG</sub></b>	<b>38.1<sup>c</sup> ± 0.0</b>	<b>23.6<sup>e</sup> ± 0.0</b>	<b>8.6<sup>f</sup> ± 0.0</b>	<b>29.7<sup>e</sup> ± 0.0</b>
<b>S3(PO)<sub>BG</sub></b>	<b>37.5<sup>e</sup> ± 0.0</b>	<b>23.4<sup>f</sup> ± 0.0</b>	<b>9.1<sup>cd</sup> ± 0.0</b>	<b>30.0<sup>d</sup> ± 0.0</b>
S3(SO) <sub>BG</sub>	35.5 <sup>h</sup> ± 0.0	24.6 <sup>c</sup> ± 0.0	9.6 <sup>b</sup> ± 0.0	30.3 <sup>c</sup> ± 0.0
S3(MO) <sub>BG</sub>	38.1 <sup>c</sup> ± 0.0	23.6 <sup>e</sup> ± 0.0	8.6 <sup>f</sup> ± 0.1	29.8 <sup>de</sup> ± 0.0
<b>S4(RO)<sub>BG</sub></b>	<b>38.0<sup>c</sup> ± 0.0</b>	<b>23.5<sup>e</sup> ± 0.0</b>	<b>8.8<sup>de</sup> ± 0.0</b>	<b>29.7<sup>e</sup> ± 0.0</b>
<b>S4(PO)<sub>BG</sub></b>	<b>37.9<sup>d</sup> ± 0.0</b>	<b>23.2<sup>g</sup> ± 0.0</b>	<b>9.0<sup>d</sup> ± 0.0</b>	<b>29.9<sup>d</sup> ± 0.0</b>
S4(SO) <sub>BG</sub>	33.4 <sup>i</sup> ± 0.0	26.1 <sup>a</sup> ± 0.1	10.1 <sup>a</sup> ± 0.0	30.5 <sup>b</sup> ± 0.0
S4(MO) <sub>BG</sub>	38.2 <sup>bc</sup> ± 0.0	23.9 <sup>d</sup> ± 0.1	8.7 <sup>e</sup> ± 0.0	29.2 <sup>g</sup> ± 0.0
B1 <sub>BG</sub>	38.0 <sup>c</sup> ± 0.0	23.0 <sup>h</sup> ± 0.0	8.9 <sup>de</sup> ± 0.0	30.0 <sup>d</sup> ± 0.0
B2 <sub>BG</sub>	37.6 <sup>de</sup> ± 0.0	23.5 <sup>f</sup> ± 0.0	9.2 <sup>c</sup> ± 0.0	29.7 <sup>e</sup> ± 0.0
<b>B3(RO)<sub>BG</sub></b>	<b>38.0<sup>c</sup> ± 0.0</b>	<b>24.0<sup>d</sup> ± 0.0</b>	<b>8.6<sup>f</sup> ± 0.0</b>	<b>29.4<sup>f</sup> ± 0.0</b>
<b>B3(PO)<sub>BG</sub></b>	<b>39.4<sup>a</sup> ± 0.0</b>	<b>25.2<sup>b</sup> ± 0.0</b>	<b>5.7<sup>g</sup> ± 0.0</b>	<b>31<sup>a</sup> ± 0.0</b>
B3(SO) <sub>BG</sub>	37.9 <sup>d</sup> ± 0.0	23.9 <sup>d</sup> ± 0.0	8.7 <sup>e</sup> ± 0.0	29.5 <sup>f</sup> ± 0.0
B3(MO) <sub>BG</sub>	38.0 <sup>c</sup> ± 0.0	23.2 <sup>g</sup> ± 0.0	8.7 <sup>e</sup> ± 0.0	30.1 <sup>c</sup> ± 0.0
<b>B4(RO)<sub>BG</sub></b>	<b>36.4<sup>f</sup> ± 0.0</b>	<b>23.0<sup>h</sup> ± 0.0</b>	<b>10.1<sup>a</sup> ± 0.0</b>	<b>30.5<sup>b</sup> ± 0.0</b>
<b>B4(PO)<sub>BG</sub></b>	<b>36.0<sup>g</sup> ± 0.0</b>	<b>23.9<sup>d</sup> ± 0.0</b>	<b>9.3<sup>c</sup> ± 0.0</b>	<b>30.8<sup>a</sup> ± 0.0</b>
B4(SO) <sub>BG</sub>	38.4 <sup>b</sup> ± 0.0	23.4 <sup>f</sup> ± 0.0	8.6 <sup>e</sup> ± 0.0	29.6 <sup>f</sup> ± 0.0
B4(MO) <sub>BG</sub>	37.8 <sup>d</sup> ± 0.0	23.1 <sup>gh</sup> ± 0.0	8.7 <sup>e</sup> ± 0.0	30.4 <sup>b</sup> ± 0.0

695 **Table 3c**

	$\beta$ -sheets	unordered	$\alpha$ -helix	$\beta$ -turns
S1 <sub>AG</sub>	50.5 <sup>c</sup> ± 0.0	17.5 <sup>d</sup> ± 0.0	11 <sup>c</sup> ± 0.0	21 <sup>e</sup> ± 0.0
S2 <sub>AG</sub>	51.00 <sup>bc</sup> ± 0.0	17.3 <sup>d</sup> ± 0.0	8.9 <sup>e</sup> ± 0.0	22.8 <sup>d</sup> ± 0.0
S3(RO) <sub>AG</sub>	<b>50<sup>cd</sup></b> ± 0.1	17.4 <sup>d</sup> ± 0.0	12.3 <sup>a</sup> ± 0.0	20.3 <sup>ef</sup> ± 0.0
S3(PO) <sub>AG</sub>	<b>50<sup>cd</sup></b> ± 0.1	18.5 <sup>c</sup> ± 0.0	11.3 <sup>bc</sup> ± 0.0	20.2 <sup>ef</sup> ± 0.0
S3(SO) <sub>AG</sub>	49.6 <sup>d</sup> ± 0.0	18.8 <sup>bc</sup> ± 0.0	11 <sup>c</sup> ± 0.0	20.5 <sup>ef</sup> ± 0.0
S3(MO) <sub>AG</sub>	49.9 <sup>d</sup> ± 0.0	17.8 <sup>cd</sup> ± 0.0	11.2 <sup>bc</sup> ± 0.0	21.1 <sup>e</sup> ± 0.0
S4(RO) <sub>AG</sub>	<b>50.8<sup>bc</sup></b> ± 0.0	16.4 <sup>ef</sup> ± 0.0	10.8 <sup>cd</sup> ± 0.0	21.9 <sup>de</sup> ± 0.0
S4(PO) <sub>AG</sub>	<b>50.3<sup>c</sup></b> ± 0.0	18.6 <sup>bc</sup> ± 0.0	10.9 <sup>cd</sup> ± 0.0	20.2 <sup>ef</sup> ± 0.0
S4(SO) <sub>AG</sub>	49.4 <sup>de</sup> ± 0.0	19.2 <sup>b</sup> ± 0.0	10.1 <sup>d</sup> ± 0.0	21.3 <sup>de</sup> ± 0.0
S4(MO) <sub>AG</sub>	47.9 <sup>e</sup> ± 0.0	19.2 <sup>b</sup> ± 0.0	11 <sup>c</sup> ± 0.0	21.8 <sup>de</sup> ± 0.0
B1 <sub>AG</sub>	48.1 <sup>e</sup> ± 0.0	16.8 <sup>e</sup> ± 0.0	12.5 <sup>a</sup> ± 0.0	22.5 <sup>d</sup> ± 0.0
B2 <sub>AG</sub>	47.5 <sup>f</sup> ± 0.0	16.9 <sup>e</sup> ± 0.0	11.7 <sup>b</sup> ± 0.0	23.8 <sup>c</sup> ± 0.0
B3(RO) <sub>AG</sub>	<b>51.5<sup>b</sup></b> ± 0.0	17.8 <sup>cd</sup> ± 0.0	5.8 <sup>g</sup> ± 0.2	24.9 <sup>b</sup> ± 0.0
B3(PO) <sub>AG</sub>	<b>51.3<sup>b</sup></b> ± 0.0	17.6 <sup>cd</sup> ± 0.0	5.1 <sup>h</sup> ± 0.0	26.1 <sup>a</sup> ± 0.0
B3(SO) <sub>AG</sub>	49.4 <sup>de</sup> ± 0.0	18.7 <sup>c</sup> ± 0.0	10 <sup>de</sup> ± 0.0	21.8 <sup>de</sup> ± 0.0
B3(MO) <sub>AG</sub>	50 <sup>cd</sup> ± 0.0	18.4 <sup>c</sup> ± 0.0	11 <sup>c</sup> ± 0.0	20.5 <sup>ef</sup> ± 0.0
B4(RO) <sub>AG</sub>	<b>51.9<sup>ab</sup></b> ± 0.0	16.3 <sup>f</sup> ± 0.0	8.1 <sup>f</sup> ± 0.0	23.7 <sup>c</sup> ± 0.0
B4(PO) <sub>AG</sub>	<b>52.1<sup>a</sup></b> ± 0.0	17.5 <sup>d</sup> ± 0.0	4.9 <sup>h</sup> ± 0.0	25.5 <sup>ab</sup> ± 0.0
B4(SO) <sub>AG</sub>	50.1 <sup>cd</sup> ± 0.0	18.5 <sup>c</sup> ± 0.0	8.4 <sup>ef</sup> ± 0.1	23.1 <sup>d</sup> ± 0.0
B4(MO) <sub>AG</sub>	49.8 <sup>d</sup> ± 0.0	20 <sup>a</sup> ± 0.0	10.3 <sup>d</sup> ± 0.0	19.9 <sup>f</sup> ± 0.0

696 Different small letters (a, b, c, d, e, f, g, and h) represent statistical differences between different storage days ( $p < 0.05$ ); AG: after  
697 gelatinization; RO, PO, SO and MO: rapeseed oil, palm oil sunflower oil and mixture oil (60 % of sunflower oil), respectively.

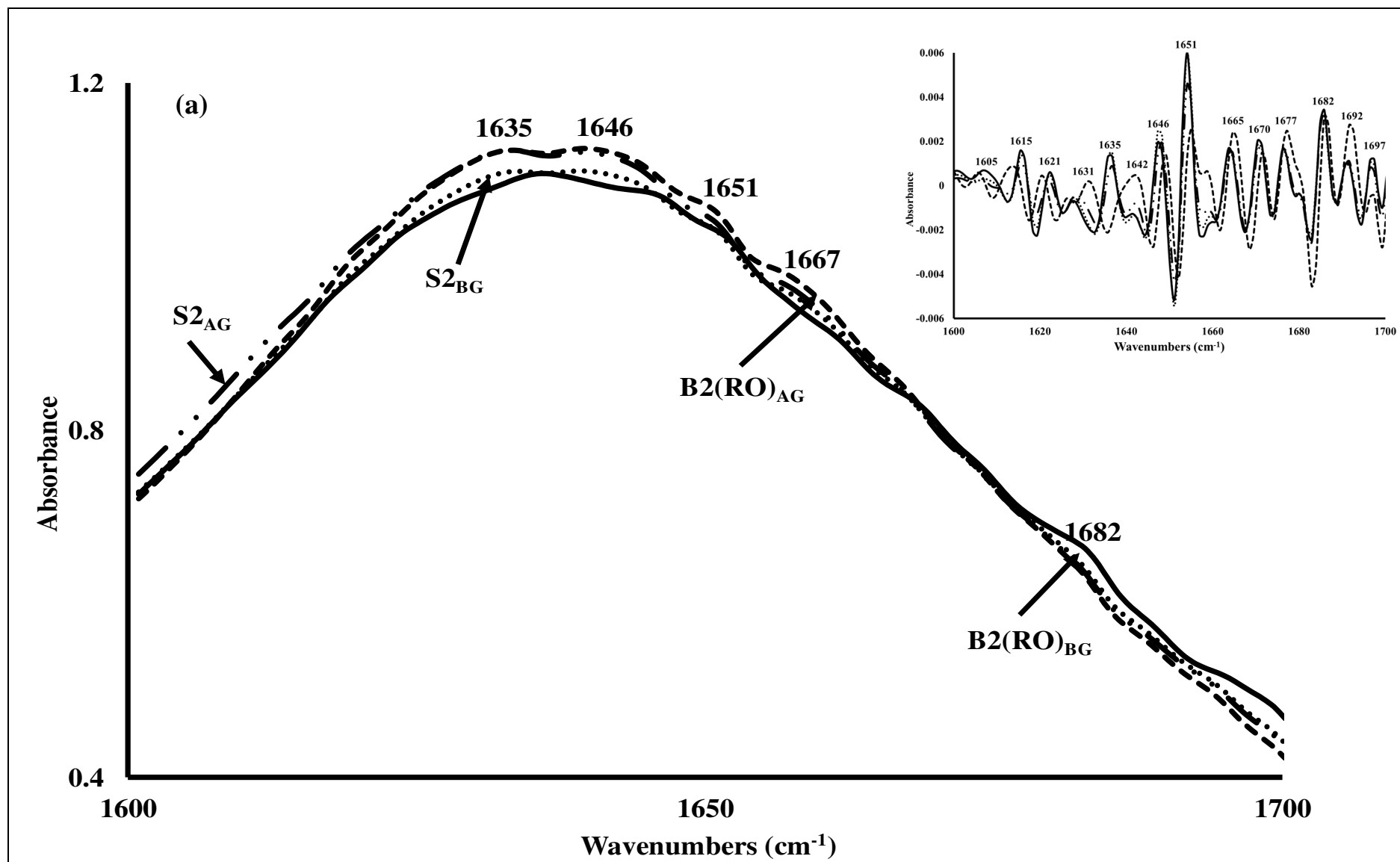
698

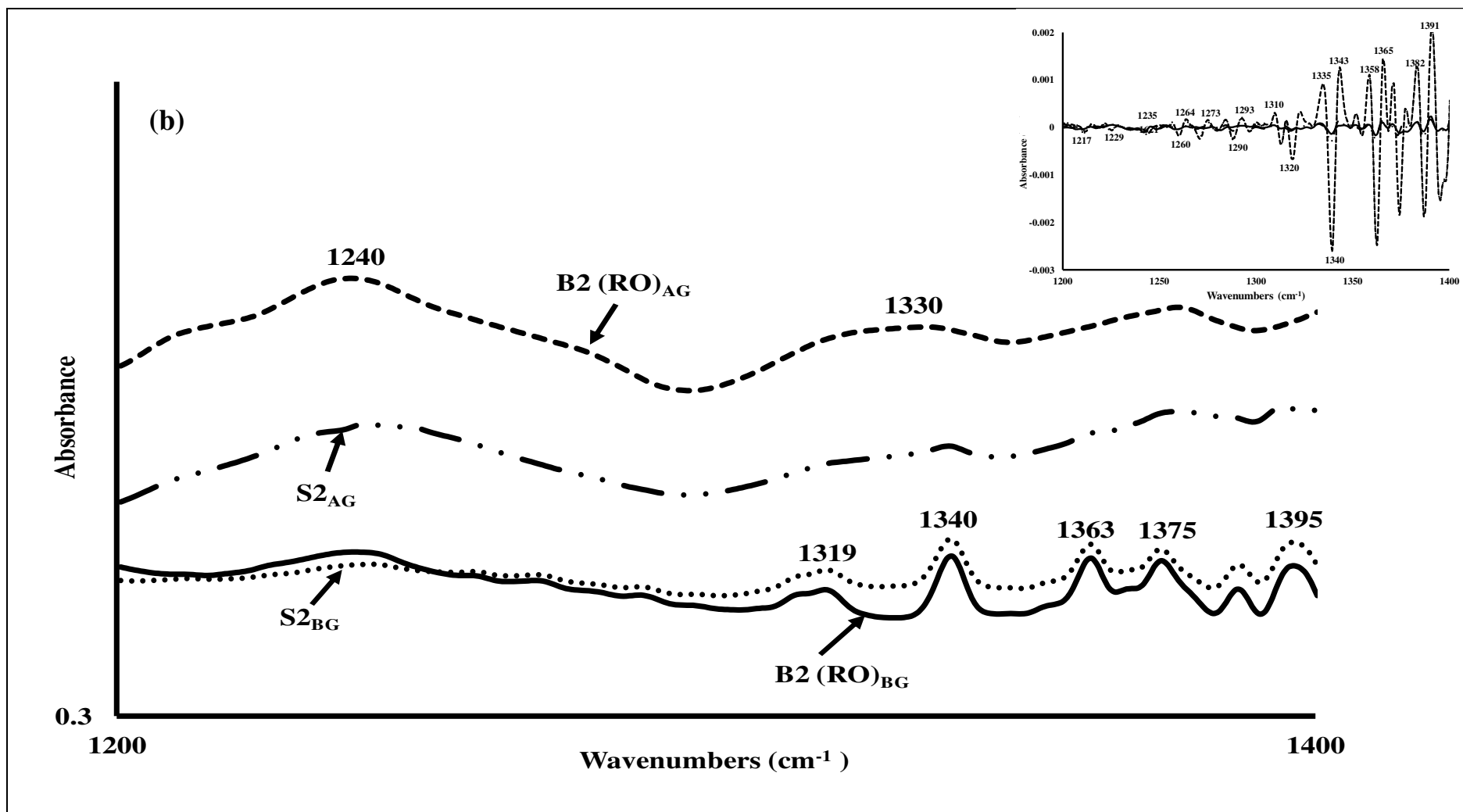
699 **Table 3d**

	$\beta$ -sheets	unordered	$\alpha$ -helix	$\beta$ -turns
S1 <sub>AG</sub>	29.7 <sup>f</sup> ± 0.0	23.9 <sup>b</sup> ± 0.0	17.7 <sup>e</sup> ± 0.0	28.7 <sup>e</sup> ± 0.0
S2 <sub>AG</sub>	26.8 <sup>i</sup> ± 0.0	26.4 <sup>a</sup> ± 0.0	15.5 <sup>h</sup> ± 0.0	31.3 <sup>b</sup> ± 0.0
<b>S3(RO)<sub>AG</sub></b>	<b>30.1<sup>de</sup> ± 0.0</b>	<b>23.2<sup>d</sup> ± 0.0</b>	<b>19.0<sup>a</sup> ± 0.0</b>	<b>27.7<sup>h</sup> ± 0.0</b>
<b>S3(PO)<sub>AG</sub></b>	<b>30.1<sup>de</sup> ± 0.0</b>	<b>23.1<sup>d</sup> ± 0.0</b>	<b>18.4<sup>c</sup> ± 0.0</b>	<b>28.4<sup>f</sup> ± 0.0</b>
S3(SO) <sub>AG</sub>	31.1 <sup>a</sup> ± 0.0	22.8 <sup>e</sup> ± 0.0	18.8 <sup>ab</sup> ± 0.0	27.4 ± 0.0
S3(MO) <sub>AG</sub>	30.0 <sup>e</sup> ± 0.0	23.4 <sup>c</sup> ± 0.0	17.2 <sup>f</sup> ± 0.0	29.3 <sup>d</sup> ± 0.0
<b>S4(RO)<sub>AG</sub></b>	<b>30.7<sup>c</sup> ± 0.0</b>	<b>23.0<sup>d</sup> ± 0.0</b>	<b>18.9<sup>ab</sup> ± 0.0</b>	<b>27.5<sup>h</sup> ± 0.1</b>
<b>S4(PO)<sub>AG</sub></b>	<b>30.4<sup>d</sup> ± 0.1</b>	<b>23.3<sup>d</sup> ± 0.0</b>	<b>18.7<sup>b</sup> ± 0.0</b>	<b>27.6<sup>h</sup> ± 0.0</b>
S4(SO) <sub>AG</sub>	29.6 <sup>f</sup> ± 0.0	23.7 <sup>bc</sup> ± 0.0	18.3 <sup>c</sup> ± 0.0	28.3 <sup>f</sup> ± 0.0
S4(MO) <sub>AG</sub>	30.0 <sup>e</sup> ± 0.0	23.6 <sup>b</sup> ± 0.0	17.4 <sup>f</sup> ± 0.0	29.0 <sup>de</sup> ± 0.0
B1 <sub>AG</sub>	29.4 <sup>g</sup> ± 0.0	23.5 <sup>c</sup> ± 0.0	19.0 <sup>a</sup> ± 0.0	28.0 <sup>g</sup> ± 0.0
B2 <sub>AG</sub>	29.4 <sup>g</sup> ± 0.0	23.4 <sup>c</sup> ± 0.0	19.0 <sup>a</sup> ± 0.0	28.1 <sup>g</sup> ± 0.0
<b>B3(RO)<sub>AG</sub></b>	<b>31.1<sup>b</sup> ± 0.1</b>	<b>22.8<sup>e</sup> ± 0.1</b>	<b>18.0<sup>d</sup> ± 0.1</b>	<b>28.1<sup>g</sup> ± 0.0</b>
<b>B3(PO)<sub>AG</sub></b>	<b>30.3<sup>d</sup> ± 0.01</b>	<b>23.4<sup>c</sup> ± 0.0</b>	<b>18.0<sup>d</sup> ± 0.0</b>	<b>28.3<sup>f</sup> ± 0.0</b>
B3(SO) <sub>AG</sub>	31.2 <sup>a</sup> ± 0.0	22.7 <sup>e</sup> ± 0.0	17.6 <sup>e</sup> ± 0.0	28.5 <sup>f</sup> ± 0.0
B3(MO) <sub>AG</sub>	30.3 <sup>d</sup> ± 0.0	23.0 <sup>d</sup> ± 0.0	17.8 <sup>e</sup> ± 0.0	28.9 <sup>e</sup> ± 0.1
<b>B4(RO)<sub>AG</sub></b>	<b>29.8<sup>ef</sup> ± 0.0</b>	<b>24.0<sup>b</sup> ± 0.0</b>	<b>16.5<sup>g</sup> ± 0.0</b>	<b>29.7<sup>c</sup> ± 0.0</b>
<b>B4(PO)<sub>AG</sub></b>	<b>29.0<sup>h</sup> ± 0.0</b>	<b>24.0<sup>b</sup> ± 0.0</b>	<b>15.1<sup>i</sup> ± 0.0</b>	<b>31.9<sup>a</sup> ± 0.0</b>
B4(SO) <sub>AG</sub>	30.8 <sup>c</sup> ± 0.0	22.8 <sup>e</sup> ± 0.0	18.7 <sup>c</sup> ± 0.0	27.7 ± 0.0
B4(MO) <sub>AG</sub>	30.2 <sup>d</sup> ± 0.0	23.1 <sup>d</sup> ± 0.0	17.1 <sup>f</sup> ± 0.0	29.6 <sup>c</sup> ± 0.0

700 Different small letters (a, b, c, d, e, f, g, and h) represent statistical differences between different storage days ( $p < 0.05$ ); AG: after  
701 gelatinization; RO, PO, SO and MO: rapeseed oil, palm oil sunflower oil and mixture oil (60 % of sunflower oil), respectively.

702 Figure 1:





703

Figure 2:

